

# Interaction ramps in a trapped Bose condensate

F. E. Zimmer and Masudul Haque

Max Planck Institute for the Physics of Complex Systems, Nöthnitzer Str. 38, 01187 Dresden, Germany

Non-adiabatic interaction ramps are considered for trapped Bose-Einstein condensates. The deviation from adiabaticity is characterized through the heating or residual energy produced during the ramp. We find that the dependence of the heat on the ramp time is very sensitive to the ramp protocol. We explain features of this dependence through a single-parameter effective description based on the dynamics of the condensate size.

Adiabaticity is a ubiquitous concept in quantum dynamics. With the advent of novel non-equilibrium experimental possibilities, *deviations* from adiabaticity in slow parameter changes have attracted a lot of attention [1–9]. The question of non-adiabaticity is of fundamental interest, but also has practical implications. Many experimental protocols involve adiabatically changing a parameter in order to reach a desired quantum state. Since non-adiabatic heating can rarely be completely avoided, it is essential to understand deviations from adiabaticity in slow ramps. In addition, the proposal of *adiabatic quantum computation* [10] raises the question of how a realistic parameter ramp in a quantum many-particle system deviates from adiabaticity. While the effect of quantum critical points in the ramp path has been considered in much detail [1, 2], first realizations of such a quantum computer will presumably be mesoscopic rather than macroscopic, without true quantum critical points. Understanding non-adiabatic ramps in *finite* quantum systems is therefore vital. A few studies of ramps in finite and trapped systems have appeared in the very recent literature [6–9], indicating an emerging recognition of the importance of this issue.

Thus motivated, in this work we consider non-adiabatic ramps in the most emblematic physical system in the world of laser-cooled atoms, namely, an interacting Bose-Einstein condensate in a harmonic trap. We consider ramps of the contact interaction from an initial value  $U_i$  to a final value  $U_f$ , occurring in time scale  $\tau$ . By varying  $\tau$ , we interpolate between the limits of the *instantaneous quench* ( $\tau = 0$ ) and the *adiabatic ramp* ( $\tau \rightarrow \infty$ ). For finite  $\tau$ , we study deviations from adiabaticity through the heating  $Q$ , which we define as the final energy at time  $t > \tau$  minus the ground state energy of the final Hamiltonian. This quantity is also called the residual energy or the excess energy [3–6], and may be thought of as the “friction” due to imperfect adiabaticity [11].

We find that the residual energy  $Q$  decreases with  $\tau$  as a power law  $Q \sim \tau^{-\nu}$  rather than exponentially, with the exponent  $\nu$  depending on the shape of the ramp. For certain ramp shapes,  $Q(\tau)$  has oscillations superposed on top of the power-law decay. The oscillation frequency is given by the breathing-mode frequency set by the harmonic trap. In contrast to most studies of the heat function  $Q(\tau)$ , we have found a simple physical description of the features of  $Q(\tau)$ . A natural description of trapped dynamics is through a variational wave function where the extent (radius) of the condensate is treated as a time-dependent variational parameter. We find that such a “radius dynamics” description reproduces the residual energy

behavior surprisingly well.

We use the Gross-Pitaevskii (GP) description [13, 14] of condensates in an isotropic harmonic trap  $V_{\text{tr}}(r)$ . The GP energy functional is

$$E[\psi] = \int_r \psi^*(r) \left[ -\frac{\hbar^2}{2m} \nabla^2 \right] \psi(r) + \frac{1}{2} U(t) \int_r |\psi(r)|^4 + \int_r V_{\text{tr}}(r) |\psi(r)|^2.$$

Here  $r$  is the radial position variable, and  $\int_r \equiv \int d^D r$  is the spatial integral appropriate to the dimensionality  $D$  of the system. The time-dependent parameter  $U$  is the effective interaction strength whose relation to the physical interaction is also  $D$ -dependent (c.f. Ref. [12] for 1D). From here on we will use trap units, expressing lengths in units of trap oscillator length and time in units of inverse trapping frequency. The condensate dynamics is given by the time-dependent GP equation,  $i \frac{\partial \psi}{\partial t} = -\frac{1}{2} \nabla^2 \psi + \frac{1}{2} r^2 \psi + U(t) |\psi|^2 \psi$ .

The GP equation provides an excellent account of many aspects of trapped condensate dynamics. We restrict ourselves to GP dynamics, which is already too rich to be studied exhaustively. While physics beyond GP is more important in lower dimensions, we will treat 1D, 2D and 3D cases on an equal footing. The questions we address are conceptually interesting irrespective of dimensionality. We will also show that the dominant effects we encounter and analyze are quite insensitive to  $D$ .

*Ramp shapes* — We analyze ramps of the form

$$U(t) = U_i + \theta(t) (U_f - U_i) r(t/\tau).$$

The ramp function  $r(x)$  starts at  $r(0) = 0$  and ends at  $r(\infty) = 1$ . We do not require  $r(x > 1) = 1$ , i.e., the ramps take place over time scale  $\tau$  but do not necessarily end at  $t = \tau$ . (Contrast, e.g., Ref. [4].)

Specifically, we consider the following forms for  $r(x)$ :

$$\begin{array}{ll} [1A] & x \theta(1-x) + \theta(x-1) & [1B] & 1 - e^{-x} \\ [2A] & x^2 \theta(1-x) + \theta(x-1) & [2B] & 1 - e^{-x^2} \\ [3A] & x^3 \theta(1-x) + \theta(x-1) & [3B] & 1 - e^{-x^3} \end{array}$$

Each [A], [B] pair has the same initial behavior,  $r(x) \sim x^\alpha$ , but the [B] versions have no endpoint kinks. Ramp shapes [1A] and [1B] ([2A] and [2B]) are compared in Figure 1a (1b).

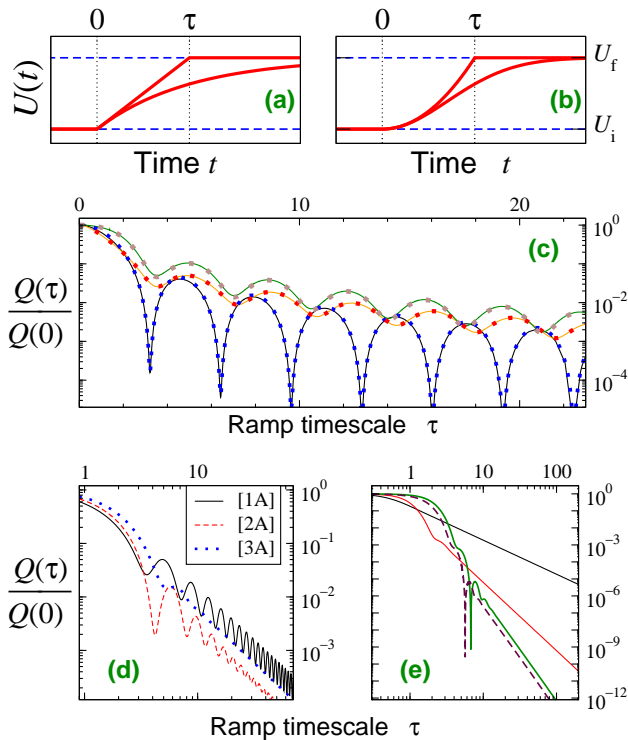


FIG. 1: (a&b) Ramp shapes [1A], [1B], & [2A], [2B]. (c-e) Some residual energy curves  $Q(\tau)$ . (c) For ramp shape [1A], Comparing full Gross-Pitaevskii results (full curves) with single-parameter variational results (dotted curves). The three pairs have  $(U_i, U_f)$  values  $(0,1)$ ,  $(10,100)$ , and  $(20,0.2)$ , from bottom to top. (d) With  $(U_i, U_f) = (10,100)$ , comparing the discontinuous-derivative ramp shapes [1A], [2A], [3A]. (e) With  $(U_i, U_f) = (20,0.2)$ , comparing  $Q(\tau)$  for smoothed ramp shapes, [1B], [2B], [3B], from smaller to larger slopes.

*Residual energy features* — In Figure 1c-e we present the behavior of the heat function  $Q(\tau)$ , normalized against its instantaneous-quench value  $Q(\tau = 0)$ .

Figure 1c shows  $Q(\tau)/Q(0)$  for several ramps of type [1A] (linear quench). The heating displays oscillations with  $\tau$ , on top of a power-law decay. The frequency of these oscillations is the same as the frequency of breathing-mode oscillations in real time. Also shown, in each case, is  $Q(\tau)/Q(0)$  found from a single-parameter variational ansatz where the cloud radius is the only variable. The near-perfect agreement indicates that the physics of heating in interaction ramps is almost completely described by the radius dynamics. In the rest of the article, we therefore present results and analysis mostly based on the variational description.

In Figure 1d, the residual energy curves are compared for the ramp shapes  $r(x) \sim x^\alpha$  with discontinuous derivatives at endpoints, [1A], [2A], [3A]. Each curve has an overall power-law decay with the same decay exponent,  $Q(\tau) \sim \tau^{-2}$ . This suggests that the residual energy for such ramps is primarily set by the endpoint kink. Superposed on the power-law decay are oscillations, more prominent for the linear quench  $\alpha = 1$  and barely visible for  $\alpha = 3$ .

In Figure 1e we focus on smoothed ramps [1B], [2B], [3B], which lead to non-oscillating decay of the residual energy. The decay exponent is seen to depend on the power  $\alpha$  of  $r(x) \sim x^\alpha$ , namely,  $Q(\tau) \sim \tau^{-2\alpha}$ .

The dimensionality does not affect the decay exponents. The  $Q(\tau)$  data shown in Figures 1c-e are for  $D = 1$ , except for the dashed curve in 1e, which is for  $D = 3$  and ramp [3B]. Comparison with the corresponding  $D = 1$  solid curve demonstrates that the  $Q(\tau)$  behavior is practically identical in different dimensions.

*Single-parameter variational description* — We formulate the radius description in terms of a Gaussian variational ansatz, which for 1D is

$$\psi(x, t) = \frac{1}{[\sqrt{\pi}\sigma(t)]^{1/2}} \exp \left[ -\frac{x^2}{2[\sigma(t)]^2} - i\beta(t)x^2 \right]. \quad (1)$$

For  $D > 1$  the variational wave function is a product of one such Gaussian factor for each dimension. Using this ansatz in the GP Lagrangian, we get the evolution equations for the variational parameters  $\sigma(t)$  and  $\beta(t)$  [15]. We could just as well use a Thomas-Fermi instead of Gaussian profile; however the results are very similar and do not substantially affect any of the arguments we make in this work. The two parameters turn out to be not independent but simply related ( $\beta(t) \propto \partial_t \ln \sigma(t)$ ). There is thus effectively a single dynamical parameter describing the system, namely the cloud radius  $\sigma(t)$ . The equation of motion for  $\sigma$  is

$$\sigma \frac{d^2\sigma}{dt^2} + \sigma^2 - \frac{1}{\sigma^2} - \frac{U(t)}{(\sqrt{2\pi}\sigma)^D} = 0, \quad (2)$$

and the energy is

$$E[\sigma] = \frac{D}{4} \left[ \frac{1}{\sigma^2} + \sigma^2 + \left( \frac{d\sigma}{dt} \right)^2 \right] + \frac{U(t)}{2(\sqrt{2\pi}\sigma)^D}. \quad (3)$$

The radius description based on the above two equations is suitable for describing breathing-mode oscillations. For constant  $U$ , trying small-amplitude oscillatory solutions of form  $\sigma = R_0 + \rho \sin(\Omega t)$ , Eq. (2) yields  $\Omega \sim \sqrt{D+2}$  for the breathing mode frequency at large  $U$ . We also find that  $R_0$  satisfies the stationary equation for the radius, i.e., that  $R_0[U] \sim U^{1/(D+2)}$  in the Thomas-Fermi limit of large  $U$ . Also, Eq. (3) shows that the excitation energy with a breathing-mode oscillation of amplitude  $\rho$  scales as  $\sim \rho^2$  with the oscillation amplitude  $\rho$ ; we will use this for our energy analysis below.

*Radius dynamics interpretation* — We now proceed to explain the  $Q(\tau)$  behaviors presented above, in terms of radius dynamics. Figure 2 (top row) shows the radius evolving as a function of time for various ramp shapes, for reasonably large  $\tau$ . In the center and bottom rows, we show the deviation of  $\sigma(t)$  from the equilibrium radius corresponding to the instantaneous value of the interaction,  $R_0(t) = R_0[U(t)]$ . For a truly adiabatic ramp,  $\sigma(t)$  would follow  $R_0(t)$  exactly; therefore the deviation  $f(t) = \sigma(t) - R_0(t)$  is at the heart of non-adiabaticity and the behavior of this quantity determines the

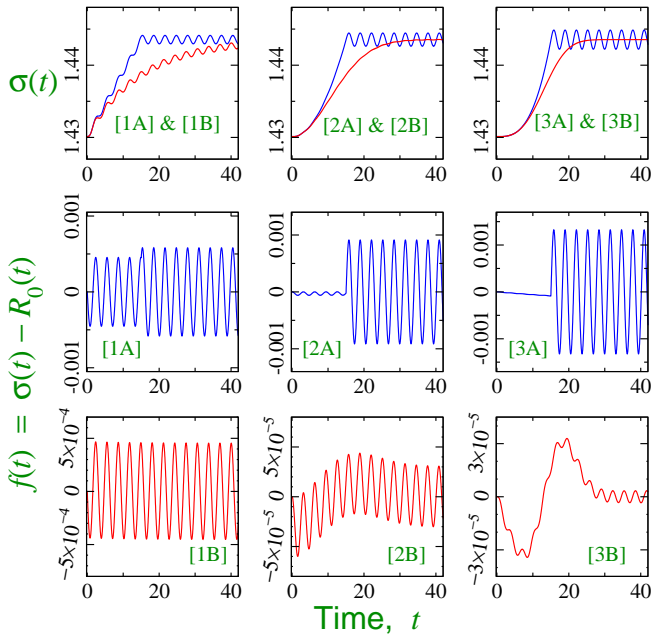


FIG. 2: Top row: condensate radius dynamics  $\sigma(t)$  for various ramp shapes,  $\tau = 15$ . Center and lower rows: deviation  $f(t)$  from the ‘instantaneous’ ground-state radius  $R_0(t)$ . Dimensions  $D = 2$ ,  $(U_i, U_f) = (20, 21)$ .

amount of heating. After the ramp, the  $f(t)$  function is purely oscillatory; the heating scales as the square of the oscillation magnitude. Figure 2 presents radius dynamics for  $D = 2$ ; the 1D and 3D cases are very similar.

For the [A] ramps with derivative discontinuities (middle row), the magnitude of the final oscillations of  $f(t)$  is determined at the ramp endpoint. For the  $(t/\tau)^\alpha$  ramp, the oscillation magnitude is  $\mathcal{O}(\tau^{-\alpha})$  during the ramp, and turns into  $\mathcal{O}(\tau^{-1})$  after the endpoint kink. For  $\alpha > 1$ , the final  $\mathcal{O}(\tau^{-1})$  oscillation is parametrically larger than the during-ramp  $\mathcal{O}(\tau^{-\alpha})$  oscillation.

We will first explain the  $\sim \tau^{-1}$  scaling of oscillations initiated at the kink. If we neglect the smaller oscillations at  $t < \tau$ , the radius  $\sigma(t) \approx R_0(t)$  at the kink  $t = \tau$  has ‘correct’ value for  $U = U_f$ , i.e.  $f$  is negligible. However the derivative is nonzero,  $\sigma'(t) \approx R_0'(t)|_{t=\tau}$ , which scales as  $\sim \tau^{-1}$ . Thus we have the following ‘initial’ conditions at  $t = \tau^+$  for subsequent evolution:  $f(\tau) = 0$ ,  $f'(\tau^+) = c_0 \tau^{-1}$ . Using  $f(t > \tau) \approx \rho \sin(\Omega t + \delta)$ , these initial values imply  $\rho \sim \tau^{-1}$ . This explains the  $\mathcal{O}(\tau^{-1})$  oscillation magnitude and hence  $\mathcal{O}(\tau^{-2})$  residual energy for ramps having a derivative jump at the endpoint.

The oscillations of  $Q(\tau)$  (Figure 1d) can be explained by relaxing the approximation  $f(t < \tau) \approx 0$  made above. The small oscillations of  $f(t < \tau)$  guarantee that  $\sigma'(t = \tau)$  oscillates around  $R_0'(t = \tau)$  as a function of  $\tau$ . This results in the final breathing mode amplitude  $\rho$  to oscillate around its  $\mathcal{O}(\tau^{-1})$  value as a function of  $\tau$ . Since the  $f(t < \tau)$  breathing-mode strength is smaller for larger  $\alpha$ , the oscillations of the heating with  $\tau$  are weaker for larger  $\alpha$ , as seen in

Figure 1d.

The lowest-row panels of Figure 2 focus on the smooth [B] ramps. In these cases, the breathing-mode strength ( $\sim \tau^{-\alpha}$ ) initiated at the beginning of the ramp remains unchanged; there is no kink to abruptly create larger oscillations. We therefore need only to explain the strength of oscillations at the beginning of the ramp, where  $r(t/\tau) = 1 - e^{-(t/\tau)^\alpha} \approx (t/\tau)^\alpha$ .

We first rewrite Eq. (2) as an equation for  $f(t)$ . To simplify notation, we will write this out explicitly only in the Thomas-Fermi limit,  $U_{i,f} \gg 1$ , and small oscillations,  $f(t) \ll R_0(t)$ . (The arguments can of course be modified to go beyond the Thomas-Fermi restriction. Small  $f(t)$  is guaranteed for large  $\tau$ .) We obtain

$$f''(t) + \Omega^2 f(t) + \frac{u''(t)}{(D+2)u^{\frac{D+1}{D+2}}} - \frac{(D+1)u'(t)^2}{(D+2)^2 u^{\frac{2D+3}{D+2}}} = 0, \quad (4)$$

with  $u = U/(2\pi)^{D/2}$ . The first two terms give pure oscillatory behavior (breathing mode at fixed  $u$ ); the last two terms are corrections due to time-varying interaction.

We first treat ramps with zero initial slope, i.e.,  $\alpha > 1$ . The initial conditions at  $t = 0^+$  are then  $f(0) = f'(0) = 0$ . With  $u = u_i + (\delta u)(t/\tau)^\alpha$ , the  $u''$  correction is dominant compared to the  $u'^2$  correction at  $t \ll \tau$ . The dominant correction terms take the form  $c_1/\tau^2$  for  $\alpha = 2$ , and  $c_1 t/\tau^3$  for  $\alpha = 3$ . The solutions of the resulting differential equation are linear combinations of oscillatory trigonometric functions and algebraic functions. It is straightforward to verify that the boundary conditions  $f(0) = f'(0) = 0$  force the oscillatory part to have coefficients scaling as  $\sim \tau^{-2}$  for  $\alpha = 2$  and  $\sim \tau^{-3}$  for  $\alpha = 3$ . This explains the  $Q \sim \tau^{-2\alpha}$  behavior for integer  $\alpha > 1$ .

The  $\alpha = 1$  case is slightly different. The initial condition still involves  $\sigma'(0) = 0$ , but since  $R_0(t) = [u(t)]^{1/(D+1)}$  has finite slope at  $t = 0^+$ , this now corresponds to  $f'(0^+) = -R_0'(0^+) = -c_3/\tau$ . This initial condition leads to a purely oscillatory  $f(t)$  with amplitude  $\sim \tau^{-1}$ , which explains  $Q(\tau) \sim \tau^{-2}$  for  $\alpha = 1$ .

*Beyond pure radius dynamics* — We justified our single-parameter analysis by noting that  $Q(\tau)/Q(0)$  is reproduced splendidly by such a description (Figure 1c). The GP dynamics is of course richer than this minimal description, one indication of which is that the *un-normalized* heat function  $Q(\tau)$  obtained from Eqs. (2), (3) deviates from full-GP results. Although a complete study of all aspects of shape dynamics induced in a ramp is beyond the scope of the present investigation, in Figure 3 we show some basic additional effects. After the size, the next obvious shape characteristic is the kurtosis  $\kappa$ , related to the fourth moment of a distribution, such that a gaussian has  $\kappa = 0$  and a more ‘rectangular’ (sharper-peaked) distribution has  $\kappa < 0$  ( $\kappa > 0$ ). The left panels of Figure 3 show that in a slow ramp, the kurtosis oscillates around the instantaneous equilibrium value just as the radius does. In the right panels, the large-amplitude radius oscillations after a sudden ( $\tau = 0$ ) quench is seen to vary from the single-parameter description; there are dramatic jumps of  $\kappa(t)$

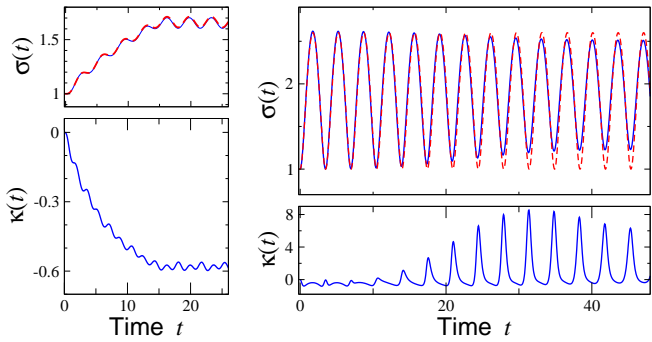


FIG. 3: Physics beyond pure radius description.  $D = 1$ ,  $(U_i, U_f) = (0, 10)$ . Left panels:  $\tau = 15$  ramp. Right panels: instantaneous quench. On top panels, radius from full GP calculations (full lines) compared to single-parameter variational calculations (dashed lines). Lower panels show kurtosis, not accessible in the radius-only description.

at the times when the  $\sigma(t)$  deviation is prominent. The energy clearly leaks from breathing-mode oscillations into other channels, even though the total energy is conserved.

*Relation to other results; Open questions* — We have addressed the fundamental question of adiabaticity in the context of a paradigm system of cold-atom physics, namely, a Bose condensate in a trap. We find that the heat function  $Q(\tau)$ , which characterizes non-adiabaticity, to have an overall power-law decay. The general intuition is that the decay of  $Q(\tau)$  should be exponential if there are no gapless points in the path of the ramp; thus finite systems are generically expected to have exponential decay, e.g., Ref. [6]. Remarkably, the GP description successfully mimics a gapless thermodynamic limit by providing power-law decay of  $Q(\tau)$ , although concepts like gap or density of states are not meaningful within the GP description.

Our result  $Q(\tau) \sim \tau^{-2\alpha}$  for smooth ramps is consistent with adiabatic perturbation theory: if our ramps are put into the form  $r(t) \sim vt^\alpha/\alpha!$ , we get  $Q(\tau) \sim \tau^{-2\alpha} \sim v^2$ , which is the generic perturbative expectation [2]. In the formulation of Ref. [4] (Sec. 3), the  $F(x)$  function for our ramp can be shown to have asymptotic form  $x^{-2\alpha}$ , which translates to an “extrinsic” contribution  $Q(\tau) \sim \tau^{-2\alpha}$ . The GP description thus retains nontrivial dynamical information pertaining to the full quantum description, despite being “merely” a nonlinear differential equation.

Another feature we have explored is the sensitivity to a final kink in the ramp shape. A recently discovered effect of such kinks is logarithmic contributions to  $Q(\tau)$  [2, 4, 16]. The effect we have found (kink induces larger oscillations over-

whelming initial excitation) is quite different. It is an open question whether or not this is unique to the present system. Oscillations of  $Q(\tau)$  are relatively poorly understood, and may well be generic in many-body ramps. In our case, it appears explicitly due to ramp shape kinks. Like other  $Q(\tau)$  features, we have provided a very physical interpretation in terms of radius oscillations. In other known examples of  $Q(\tau)$  oscillations [4–6], the physical explanation of oscillations, where known, are all different.

The present work opens up several new research avenues. Ramps in the trapping frequency should also induce radius oscillations, but details may well be different from interaction ramps. Physical insights developed in our study of  $Q(\tau)$  can perhaps be applied to better understand “optimal ramp” studies seeking to find ramp paths producing minimal heating [11]. Another natural extension of our work is a treatment of condensates beyond the GP description, e.g., truncated Wigner schemes or numerical full quantum treatments of few-boson systems.

- 
- [1] See review and citations of earlier work in: J. Dziarmaga, *Adv. Phys.* **59**, 1063 (2010); A. Polkovnikov, K. Sengupta, A. Silva, M. Vengalattore, arXiv:1007.5331v1.
  - [2] C. De Grandi, V. Gritsev, and A. Polkovnikov, *Phys. Rev. B* **81**, 012303 (2010); **81**, 224301 (2010).
  - [3] T. Caneva, R. Fazio, and G. E. Santoro, *Phys. Rev. B* **76**, 144427 (2007). F. Pellegrini, S. Montangero, G. E. Santoro, and R. Fazio, *Phys. Rev. B* **77**, 140404(R) (2008). T. Caneva, R. Fazio, and G. E. Santoro, *Phys. Rev. B* **78**, 104426 (2008).
  - [4] M. Eckstein and M. Kollar, *New J. Phys.* **12**, 055012 (2010).
  - [5] E. Canovi, D. Rossini, R. Fazio, and G. E. Santoro, *J. Stat. Mech.* (2009) P03038.
  - [6] T. Venumadhav, M. Haque, and R. Moessner; *Phys. Rev. B* **81**, 054305 (2010).
  - [7] G. Roux, *Phys. Rev. A* **81**, 053604 (2010).
  - [8] J.-S. Bernier, G. Roux, and C. Kollath, arXiv:1010.5251.
  - [9] M. Collura and D. Karevski, *Phys. Rev. Lett.* **104**, 200601 (2010).
  - [10] E. Farhi, J. Goldstone, S. Gutmann, and M. Sipser, *Science* **292**, 472 (2001); arXiv:quant-ph/0001106.
  - [11] J. G. Muga, Xi Chen, A. Ruschhaupt, and D. Guery-Odelin, *J. Phys. B* **42**, 241001 (2009).
  - [12] M. Olshanii, *Phys. Rev. Lett.* **81**, 938 (1998).
  - [13] L. P. Pitaevskii, *Sov. Phys. JETP* **13**, 451 (1961).
  - [14] E. P. Gross, *Nuovo Cimento* **20**, 454 (1961).
  - [15] V. M. Perez-Garcia, H. Michinel, J. I. Cirac, M. Lewenstein and P. Zoller, *Phys. Rev. Lett.* **77**, 5320 (1996); *Phys. Rev. A* **56**, 1424 (1997).
  - [16] B. Dóra, M. Haque, and G. Zaránd, arXiv:1011.6655.